Distinct Membrane Mechanical Properties of Human Mesenchymal Stem Cells Determined Using Laser Optical Tweezers

Igor Titushkin and Michael Cho

Department of Bioengineering, University of Illinois, Chicago, Illinois 60607

ABSTRACT   The therapeutic efficacy of mesenchymal stem cells (MSCs) in tissue engineering and regenerative medicine is determined by their unique biological, mechanical, and physicochemical characteristics, which are yet to be fully explored. Cell membrane mechanics, for example, has been shown to critically influence MSC differentiation. In this study, we used laser optical tweezers to measure the membrane mechanics of human MSCs and terminally differentiated fibroblasts by extracting tethers from the outer cell membrane. The average tether lengths were 10.6 ± 1.1 μm (hMSC) and 3.0 ± 0.5 μm (fibroblasts). The tether extraction force did not increase during tether formation, which suggests existence of a membrane reservoir intended to buffer membrane tension fluctuations. Cytoskeleton disruption resulted in a fourfold tether length increase in fibroblasts but had no effect in hMSCs, indicating weak association between the cell membrane and hMSC actin cytoskeleton. Cholesterol depletion, known to decrease lipid bilayer stiffness, caused an increase in the tether length both in fibroblasts and hMSCs, as does the treatment of cells with DMSO. We postulate that whereas fibroblasts use both the membrane rigidity and membrane-cytoskeleton association to regulate their membrane reservoir, hMSC cytoskeleton has only a minor impact on stem cell membrane mechanics.

INTRODUCTION

The mesenchymal stem cells (MSCs) isolated from adult bone marrow are able to differentiate into multiple lineages of connective tissue including bone, cartilage, tendon, fat, and muscle (1,2). When treated with appropriate growth factors in vitro, multipotent MSCs can be induced to differentiate into osteoblasts, adipocytes, and chondrocytes (3). The vast therapeutic potential of MSCs for treatment of diseases has been recognized. However, the complexity of events associated with transformation of these precursor cells leaves many unanswered questions about morphological, structural, proteomic, and functional changes in stem cells. The knowledge of MSC behavior would allow more effective approaches to cell expansion in vitro and regulation of their commitment to a specific phenotype. As reported by many authors, stem cells have quite unique structural, mechanical, and biochemical properties, which are quite different from those of fully differentiated cells (4). Mechanical properties such as cytoskeleton organization and elasticity, membrane tension, cell shape, and adhesion strength may play an important role in cell fate and differentiation (5,6). For example, dynamic arrangement of the actin network is critical in supporting the osteogenic differentiation of human MSCs (7). In addition, cell shape was shown to regulate MSC commitment to adipogenic or osteogenic lineage via cytoskeletal tension and endogenous Rho GTPase activity (8). These studies demonstrate the importance of mechanical characteristics of the cells for engineering of tissues in vitro from isolated stem cells.

Cell plasma membrane plays an important role in many cell functions including, just to name a few, proliferation, differentiation, and mitosis (9,10). It is an active and dynamic structure with numerous control mechanisms such as membrane tension and surface area regulation by membrane turnover (11). Most cells use endomembrane to continually add or delete the plasma membrane to maintain surface area homeostasis. Membrane tension is both a sensor and an effector in this process so that the membrane responds to changing mechanical stress with altered surface area. Regulation of the membrane surface area should be distinguished from the cell volume regulation, because the cell surface presented by a lipid bilayer is not just the outer limit of a cell volume but a topologically and biophysically distinct entity (12). Local and integral membrane tension is also believed to control membrane traffic, membrane-cytoskeleton attachment, endocytosis rate, cell adhesion, and motility (13–15). Due to this strong involvement of the membrane in many important cell functions, it is likely that mechanical characteristics of the membrane are also crucial for stem cell differentiation.

Detailed characterization of the membrane mechanics in mammalian cells is a challenging task due to the complex membrane structure, regulation mechanisms, and its interaction with intracellular components. Unlike simple bilayers in model lipid vesicles, cell membranes are coupled to the cell cytoskeleton and extracellular environment via molecular interactions including lipid-protein bonds, transmembrane protein linkage to cytoskeleton, and the extracellular matrix (16–19). These interactions result in more complex membrane responses to any changes in intracellular metabolism, cell microenvironment, and external stimuli. For example, cells maintain a constant membrane tension under

normal conditions, and even large osmotic swelling does not lead to a significant increase in the membrane tension (20). This rapid membrane response to accommodate morphological or osmotic changes is not simply a result of elastic stretching of the membrane that has very low expandability (21). Rather, the ability to maintain a constant membrane tension is attributed to the membrane reservoir that could buffer the fast variations in the membrane tension (11). Large and slower changes in the membrane area are believed to be mediated by tension-controlled incorporation of lipid material from internal membrane stores. The concept of a membrane reservoir was first inferred from observations of cell membrane tension during chemical or mechanical perturbations. The existence of a membrane reservoir in many cell types was subsequently proved directly based on experiments with membrane tether extraction (22). When a latex bead attached to the membrane is pulled away from the cell, a thin hollow membrane cylinder (tether) is extended from the cell to the bead. It was shown that the force required to pull the tether from neurons or fibroblasts does not change over a large range of tether lengths (20). This constant force serves as evidence that the membrane is being pulled to the tether from some available membrane depot. At some critical tether lengths, this membrane reservoir is depleted and an abrupt rise in the tether force prevents further tether elongation. The primary role of such a membrane reservoir is believed to buffer changes in the membrane tension.

Tether extraction is perhaps the most accurate method to quantitatively characterize the plasma membrane reservoir (23). To form a membrane tether, micron-sized latex beads are typically used as handles to grab the cell membrane. For tight binding to the cell surface, the beads are coated with active molecules (e.g., antibodies, extracellular matrix proteins, and lectins) via noncovalent adsorption or covalent linkage. The bead may then be manipulated by aspiration with a micropipette or by trapping it optically with laser optical tweezers (LOT). The latter technique provides a very flexible and accurate method to measure the cell membrane mechanical properties including tether formation (24,25). For example, LOT was employed to study membrane tethers in many cell types such as outer hair cells, neuronal growth cones, and molluscan neurons (22,23,26). The LOT tether extraction technique was also used to provide the first evidence of a membrane reservoir in mouse fibroblasts (21).

In this study, we seek to explore and determine the differences in the mechanical properties of the membranes of human MSCs and fibroblasts. We used LOT to extract tethers from the cell plasma membranes to characterize quantitatively the membrane reservoir and to elucidate possible mechanisms of its regulation in undifferentiated and terminally specialized cells. Detailed characterization of stem cell mechanics may help us to better understand and control the differentiation mechanisms for various stem cell-based tissue engineering and regenerative medicine applications.

MATERIALS AND METHODS

Cell culture

Human mesenchymal stem cells (hMSCs) and human fibrosarcoma cell line (HT1080) were grown in Dulbecco's modified Eagle's medium containing L-glutamine, 15% fetal bovine serum, 1% penicillin/streptomycin. The cells were maintained at 37°C in 5% CO_2. The cells were harvested with trypsin/EDTA and plated on a 22 × 22 mm coverslip 1 or 2 days before the experiment. hMSCS between passages 3–9 were used for all experiments. No effect of passage number or cell density on tether extraction was observed. Positive control experiments were performed to differentiate hMSCs into bone cells or chondrocytes using osteogenic or chondrogenic differentiation media. The molecular markers such as calcium nodules and osteocalcin (i.e., osteogenic cells) and collagen type II (i.e., chondrogenic cells) were used to verify the intended differentiation (data not shown).

For microscopic observation and optical tweezers manipulation, the coverslip with adhered cells was washed with phosphate buffered saline (PBS) and mounted on a microscope glass slide with a ~100 μm spacer. The cells between the coverslip and the slide were sealed at the edges of the coverslip. All experiments were conducted at room temperature. To study the effect of different drugs on tether formation, the cells were incubated with respective reagent solution in PBS at 37°C as follows: cytochalasin D (2 μM for 40 min), methyl-β-cyclodextrin (MβCD, 5 μM for 30 min), and dimethyl sulfoxide (DMSO, 2% for 15 min). Samples were then washed with PBS and mounted on the microscope slide as described.

Preparation of latex beads

Fluorescent polystyrene beads 0.5 μm in diameter (FluoSpheres, 515 nm emission, Molecular Probes, Eugene, OR) were used for tether extraction from the cell membrane. Mouse anti-CD29 monoclonal antibodies (Research Diagnostics, Concord, MA) were covalently coupled to carboxylate-modified bead surface via carbodiimide linkage. The standard conjugation procedure is described elsewhere (25). In brief, 200 μg of mouse anti-CD29 antibody in 200 μl MES buffer (50 mM 2-morpholinoethanesulfonic acid (MES), pH 6.0) was mixed with the same volume of 2% aqueous suspension of carboxylate-modified microspheres, and 5 mg N-(3-dimethylaminopropyl)-N'-ethyl-carbodiimide hydrochloride (EDAC, Sigma-Aldrich, St. Louis, MO) was added. After incubation on a shaker for 2 h at room temperature, the suspension was washed in PBS three times by centrifugation. After final centrifugation, the precipitate was resuspended in 1 ml of PBS containing 1% bovine serum albumin (BSA) and 2 mM sodium azide and stored at 4°C. Before each experiment, the suspension was sonicated and diluted 100 times with PBS. A coverslip with cells was incubated with a 3% BSA solution for 15 min, then 100 μl of bead suspension for 15 min at room temperature. Cells were washed in PBS and mounted on a microscope slide.

Laser optical tweezers setup, calibration, and manipulation

Cells were observed with a Nikon microscope (Eclipse E-800, Nikon, Melville, NY) in differential interference contrast, bright-field, and epifluorescence modes. The bright-field images of cells were superimposed onto the fluorescent images of the beads (455/70 nm excitation, 515 nm long-pass emission). Bright fluorescence of the beads resulted in a higher signal/noise ratio and allowed more precise bead position tracking. Infrared Nd:YAG laser (1064 nm, continuous wave, 5 W maximum output power, SpectraPhysics, Mountain View, CA) was used for particle optical trapping (Fig. 1). The laser beam was expanded 3× and directed to the microscope objective (100× PlanApo, oil immersion, numerical aperture (NA) = 1.4) by two mirrors. The laser beam was coupled to the microscope optical axis by low-pass dichroic mirror (950 nm short pass, Chroma Technology, Rockingham, VT). Two 200 mm focal length lenses were used to move the trap in the focus plane of the objective. One lens was stationary; the other one was moved in the x- and y-directions by a motorized high precision translation stage. A 16-bit
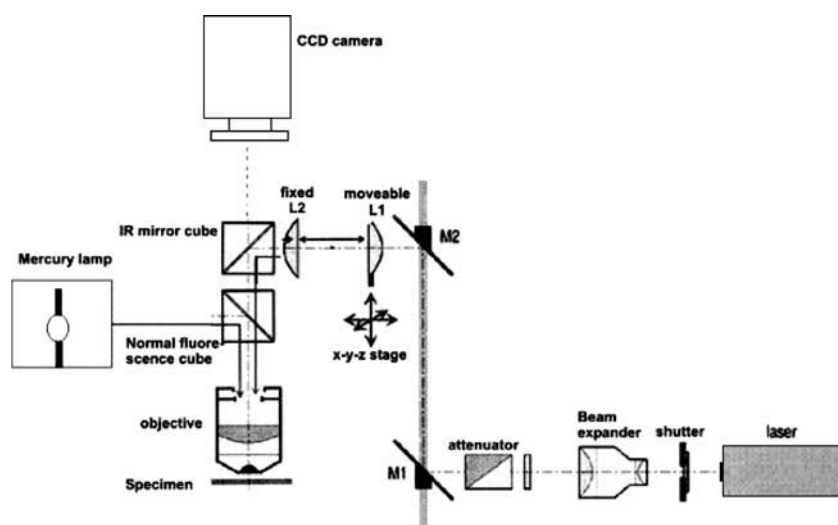
FIGURE 1 Schematic diagram of the LOT system enhanced with epifluorescence. An infrared laser beam was steered to trap and move micrometer-size particles in the specimen focal plane. The particle position is monitored with a CCD camera in bright-field and/or fluorescence modes. See text for details.

charge-coupled device (CCD) camera (Photometrics, Tucson, AZ) was used to image cells, fluorescent beads, and the laser position. The laser reflection from the coverslip was used to align optical tweezers and to monitor trap position between the experiments. Laser reflection was blocked completely during experiment by a neutral density filter located before the camera aperture window.

To measure the force applied to the bead trapped by LOT, we used an elastic spring approximation that is valid for small displacements of a trapped particle, where the trap potential is harmonic:

$$F = -k_{OT}x,$$

where k_{OT} is the stiffness of the trap and x is the particle displacement from the center of the trap. To determine the LOT stiffness, we measured thermal fluctuations of a bead caught in the trap and used the equipartition theorem to calculate the trap strength (27):

$$\frac{1}{2}k_{OT}\langle x^2 \rangle = \frac{1}{2}k_B T,$$

where k_{OT} is the trap spring constant, $\langle x^2 \rangle$ is mean-square displacement in one axis, k_B is the Boltzmann's constant, and T is the absolute temperature. The linearity of Maxwell's equations implies that the trap stiffness is linearly proportional to the laser power. The spring constant of the LOT was measured with the same beads used in experiments at different laser powers. To extract a tether from the cell membrane, a latex bead attached to the cell was chosen randomly and optically trapped. Then the bead was displaced from its equilibrium position by moving the trap away from the cell at constant speed in the range 0.5–1.5 μm/s. The bead position was monitored and recorded continuously at a 10 Hz frame rate. The tether growth was observed until the bead escaped from the trap and quickly returned to the original position. For analysis of bead motion, the bead position was tracked with nanometer-scale resolution using a MetaMorph image processor (Molecular Devices, Downingtown, PA). LOT movement plot was superimposed on a bead versus time graph as a straight line with the slope corresponding to LOT speed. From this chart, the bead displacement from the trap and the corresponding optical force were calculated. The total tether length, average tether elongation force, and maximum escape force were also determined. Typically, 35–40 beads from ~20 cells were analyzed for each experiment condition and cell type.

Cell cytoskeleton observation by laser scanning confocal microscopy

To observe the cell cytoskeleton structure, cells were fixed in 3.7% formaldehyde and permeablized in cold (−20°C) acetone for 3 min. Nonspecific

binding sites were blocked using a 3% BSA solution for 30 min at room temperature. The intracellular actin filaments were stained with rhodamin-phalloidin (5 μM) for 30 min at room temperature (Molecular Probes) and imaged by a laser scanning confocal microscope (Radiance 2001MP, Bio-Rad, Hercules, CA) and a Nikon TE2000-S inverted microscope with 60× Plan Apo objective (NA = 1.4), green HeNe laser. Emission filters (590/70 nm) were used to collect confocal images of actin microfilaments and stress fibers in untreated and cytochalasin D treated cells.

RESULTS

Dynamic membrane tether force measurement

Polystyrene beads with diameter 0.5 μm conjugated with anti-CD29 antibody were attached to the membrane and used as handles to extract plasma membrane tethers from hMSCs and fibroblasts (Fig. 2). The specificity of beads binding to β1-integrin subunits was tested with similar but not coated beads. Particles not conjugated with antibody demonstrated a very low level of binding to the cells. These results suggest high binding specificity for antibody-coated probes. An average of 10–20 particles per cell were observed bound to the cell surface in the typical experiment. Upon binding, the
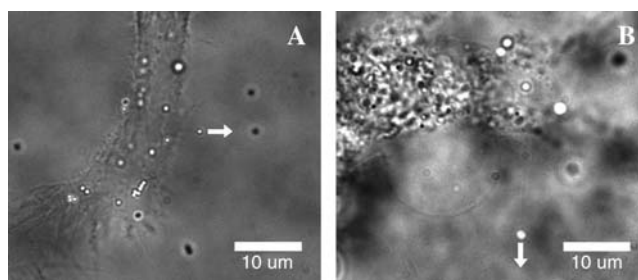

FIGURE 2 Membrane tethers extracted from fibroblasts (A) and hMSCs (B). Fluorescent beads (0.5 μm in diameter) were attached to the cell membrane and pulled away from the cell by LOT as shown with the arrows. Thin membrane tethers extending from the beads to the cell body appear as faint shadows in the bright-field/fluorescence images.

beads demonstrated two types of behavior: immobile beads and fluctuating beads. The immobile particles could not be displaced by LOT and probably were tightly anchored to the cell cytoskeleton through multiple integrin links. Alternatively, fluctuating beads were loosely bound to the membrane and often produced tethers while being dragged by LOT. The percentage of fluctuating beads depended on membrane mechanical properties and cytoskeleton integrity and varied for different cell types and drug treatment (Table 1). For example, in hMSCs more beads were mobile than in fibroblasts (34% and 19%, respectively), and this difference between the two cell types was generally observed even after various chemical treatments. We attribute this difference to the cell type-specific integrin dynamics, which depends on the membrane structural properties, and integrin interaction with cytoskeleton as illustrated by single particle tracking experiments (28,29).

A mobile bead was chosen randomly on the cell surface and pulled with LOT from its equilibrium position at a constant speed to form a thin membrane tether (Fig. 2). Only bead displacements more than 1 μm in length were classified as tethers and included in further quantitative analysis. Some tethers could be visualized as thin shadows in the bright-field image. The tether formation was proved by rapid ($\sim$0.1 s) retraction of the bead to its original position after escaping from the trap.

The time course of a typical tether pulling experiment is shown in Fig. 3. The LOT moved at a constant rate of 0.7 μm/s, as indicated by the straight line in the plot. Knowing the LOT spring constant k and bead displacement from the center of optical trap Δx, the force exerted on the bead by LOT was derived as $F = k\Delta x$. The force versus length profile (Fig. 3 B) shows that during tether elongation the force on the bead fluctuated around the constant value. When a tether reached the maximum length, the force abruptly rose until the bead escaped from the trap, indicating depletion of the membrane reservoir. If the tether elongation were due to
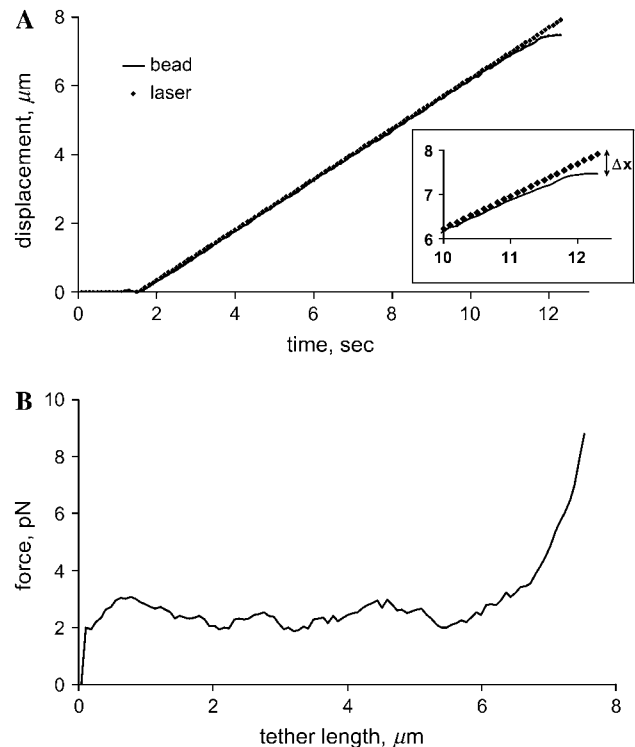

FIGURE 3 Typical tether extraction experiment. (*A*) Time course of a bead dragging by LOT. The motion of the laser tweezers with the trapped bead started at 1.5 s and continued until the bead escaped at 12 s. (*Inset*) The bead displacement from the center of the trap Δx increased rapidly during the last 2 s, indicating a sudden increase in the tether force. (*B*) Force exerted on the bead by LOT as a function of the tether length. During tether growth, force fluctuated near 3 pN, suggesting that the membrane was pulled from a reservoir. After reservoir depletion at 7 μm tether length, the force rapidly increased until the bead escaped from the trap.

TABLE 1   Average membrane tether parameters for two types of cells

Treatment	Plateau force, pN	Escape force, pN	Tether length, μm	Mobile beads, %
	HT1080 fibroblasts			
Control	3.7 ± 0.6	8.8 ± 0.5	3.0 ± 0.5	19
Cytochalasin D	3.1 ± 0.2	9.0 ± 0.6	12.7 ± 2.3	24
MβCD	3.1 ± 0.4	7.9 ± 0.4	4.9 ± 1.5	26
Ctochalasin D and MβCD	2.8 ± 0.2	8.2 ± 0.7	13.5 ± 2.1	27
DMSO	2.8 ± 0.3	8.3 ± 0.6	17.8 ± 2.7	39
	Mesenchymal stem cells			
Control	2.9 ± 0.3	9.7 ± 0.7	10.6 ± 1.1	34
Cytochalasin D	2.9 ± 0.2	8.8 ± 0.5	10.7 ± 2.0	61
MβCD	2.8 ± 0.2	8.5 ± 0.3	16.6 ± 1.9	64
Cytochalasin D and MβCD	2.6 ± 0.2	7.9 ± 0.6	17.9 ± 1.6	63
DMSO	2.6 ± 0.2	9.0 ± 0.8	17.4 ± 3.1	58

membrane stretching, the force would be expected to increase with the tether length. However, a plateau on the force-distance profile suggests that an additional membrane is drawn from a buffered reservoir. The average force in the plateau phase was 3.7 ± 0.6 pN and 2.9 ± 0.3 pN for fibroblasts and hMSCs, respectively (values statistically different at $p < 0.05$). The bead escape force is the maximum force applied by LOT at a given laser power and averaged to 9 ± 1 pN in all experiments.

The full tether length (from the start of bead pulling to its escape from the LOT) did not depend on the pull rates in the range 0.5–1.5 μm/s. At these low velocities the membrane viscosity has negligible effects on bead dynamics (30). Besides, the Stokes drag in an aqueous solution on a 0.5 μm bead at a velocity 1.5 μm/s is estimated to be <0.02 pN and thus may be disregarded in comparison with LOT force. The slower rate may also allow the membrane cytoskeleton to rearrange under a high tension, eliminating the dynamic component of cytoskeleton reorganization.

Photodamage caused by exposure to a high intensity laser radiation is considered one of the most serious limitations of

LOT. Although near infrared (1064 nm) radiation is weakly absorbed in a water environment, a high energy flux may produce temperature increases and local structural changes in cell components (31). In our experiment, each tether formation took 15–30 s. For this short time period, no mechanical or structural changes were observed, as tested by repeating the tether pulling experiment using the same bead several times at 1–2 min intervals. Tether length distributions for fibroblasts and hMSCs are shown in Fig. 4. Many long tethers, up to 30 μm, could be produced from hMSCs. In contrast, most tethers from HT1080 fibroblasts did not exceed 3 μm in length. The average tether length was 3.0 ± 0.5 μm and 10.6 ± 1.1 μm for fibroblasts and hMSCs, respectively.

Membrane-cytoskeleton interaction

Actin microfilaments are one of the most important structural components of the cell cytoskeleton, which determines the cell shape, mobility, and mechanical properties. The strong association of the cell cytoskeleton with the plasma membrane in many cell types suggests that mechanical functions of the membrane may depend on cytoskeleton organization (32,33). Confocal microscopy images revealed significant differences in the cytoskeleton arrangement in hMSCs and fibroblasts (Fig. 5). Whereas hMSCs have many thick actin stress fibers extending through the cytoplasm and ending at focal contacts on the cell basolateral surface, the actin filaments in fibroblasts are organized into a thin dense meshwork with fewer and smaller stress fibers. These two types of actin organization could reflect the differences in the specialized cell functions and may explain cell type-dependent mechanical characteristics. The thin actin network may provide significant strength and resilience to fibroblasts as predicted, for instance, by theoretical tensegrity models (34,35). Indeed, fibroblasts demonstrate a rounder and more compact morphology on two-dimensional (2D) substrates as compared to extremely thin and spread hMSCs. The strength and compli-

ance of the cell cytoskeleton may account for these morphological differences. Further differences in cytoskeleton were observed after cells were treated with cytochalasin D. Whereas thick stress fibers in hMSCs completely disappeared, some smaller actin filaments were still present at the cell periphery of fibroblasts (Fig. 5, C and D). This observation emphasizes the differences in the stability and dynamics of intracellular actin structures.

When actin microfilament polymerization was inhibited by treatment with cytochalasin D, the length of tethers extracted from fibroblasts increased more than fourfold with respect to the tether length in untreated fibroblasts. In contrast, disruption of the actin microfilaments in hMSCs evidently did not affect the tether length (Fig. 4, C and D). This result, which illustrates an important role of actin cytoskeleton in the membrane reservoir of fibroblasts, is likely due to strong interaction between the membrane and actin cytoskeleton in fibroblasts. On the other hand, we observed weak cytoskeleton-membrane interactions in hMSCs, so that alteration of cytoskeletal organization did not result in significant changes in the tether length and membrane buffering reservoir. An extensive interaction between the actin network and the membrane bilayer in fibroblasts possibly accounts for the higher average force (3.7 ± 0.6 pN) required to extract tethers in these cells compared with that for hMSCs (2.9 ± 0.3 pN). Following cytoskeleton disintegration, this force was found to decrease in fibroblasts but did not change in hMSC, which emphasizes once more the different role of cytoskeleton in the membrane mechanics of the two types of cells.

Interestingly, after stem cell treatment with cytochalasin D the percentage of fluctuating beads increased significantly (from 34% to 61% in control and treated hMSC, respectively) although tether length practically did not change (Table 1). The bead mobility increase is explained by the relaxation of integrin's physical link to the actin microfilament after cytoskeleton disruption. However, integrins are unlikely to play a
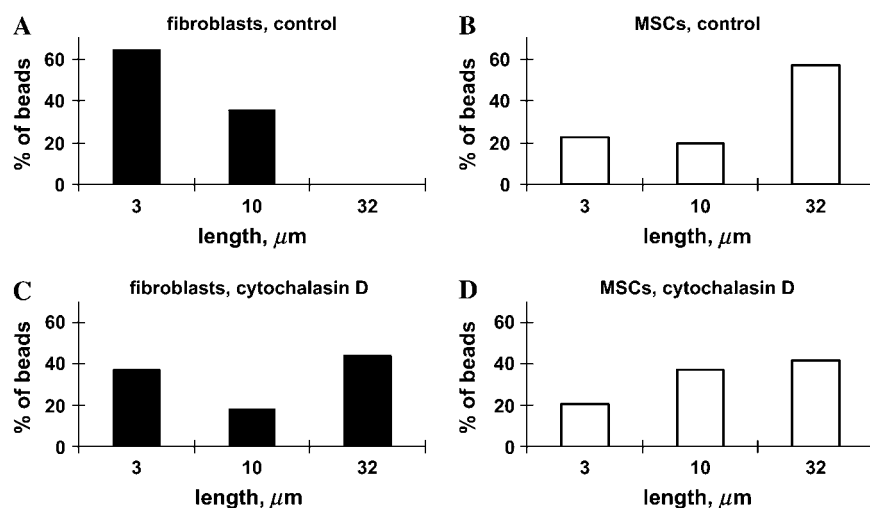

FIGURE 4 Tether length distributions for fibroblasts and hMSCS before (*A* and *B*) and after (*C* and *D*) cytoskeleton disruption with cytochalasin D. Note the dramatic increase in the tether length in fibroblasts after this treatment. Each distribution was constructed from 35 to 40 tether measurements.
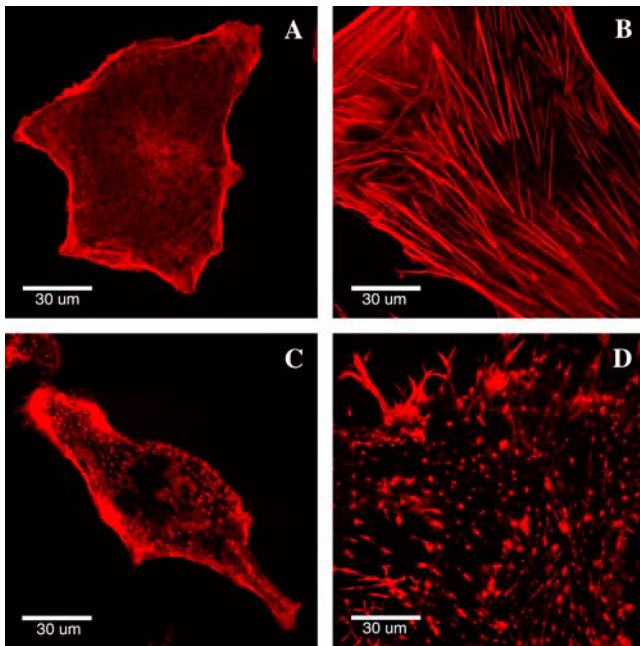
FIGURE 5   Actin cytoskeleton organization in fibroblasts (*A*) and hMSCs (*B*). hMSCs are typically bigger in size than fibroblasts and have many thick actin stress fibers. Microfilaments were disrupted using cytochalasin D in fibroblasts (*C*) and MSCs (*D*).
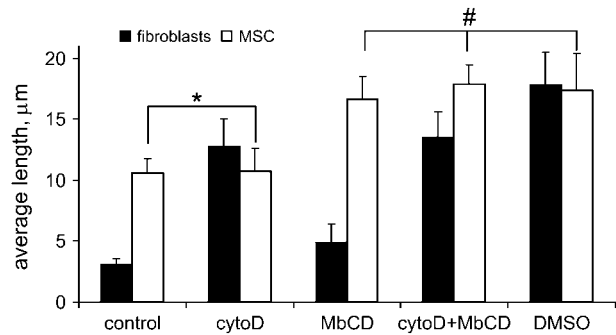

FIGURE 6   Effect of different drug treatments on the average tether length in fibroblasts and hMSCs. For each type of cell, control case was significantly different ($p < 0.01$) from those treated with drugs. However, one exception is found in hMSCs before and after cytochalasin D treatment, where the tether length was not statistically different (marked with *). Also, no statistical difference was observed between tether length in hMSC exposed to MβCD, MβCD/CytoD, and DMSO (indicated by #). The value in each category represents the average and standard error of measurement from 35 to 40 tethers.

major role in mediating membrane-cytoskeleton adhesion, as shown by similar tether lengths before and after cytochalasin treatment.

Role of membrane rigidity in buffering reservoir size

Cholesterol is a sterol lipid that is one of the main lipid components of the plasma membrane of all mammalian cells. It is known to have a major impact on physical properties of the membrane bilayer, such as phospholipid ordering, membrane fluidity, deformability, and elastic modulus (36–38). We used the water-soluble cholesterol carrier MβCD to deplete cholesterol from the cell plasma membrane (39). Consistent with reduction of the cholesterol level to decrease the membrane stiffness (40,41), cholesterol depletion with MβCD in our experiments resulted in an increase of the membrane tether length. Compared to control cells, the average tether length increased 1.6-fold in both types of cells (Fig. 6). Cholesterol appears to be closely involved in the membrane dynamics and regulation of the membrane buffering reservoir in both types of cells. An increase in MβCD concentration or incubation time did not result in further significant increase in tether length. Membrane mechanical properties seem to change dramatically with initial decrease of cholesterol level. However, cholesterol content is known to influence many other membrane characteristics (e.g., lipid domains distribution) in a complex concentration-dependent fashion (42).

Simultaneous cholesterol depletion and cytoskeleton disruption have additive effects on the tether length. When the cells were treated with two drugs (MβCD and cytochalasin D), long tethers could be produced from fibroblasts and hMSCs (average tether length 14 ± 2 μm for fibroblasts and 18 ± 2 μm for hMSCs). In fact, there was only a 1.3-fold difference in tether length in hMSCs and fibroblasts after these concomitant treatments. In fibroblasts, both membrane dissociation from cytoskeleton and reduction in cholesterol-mediated membrane stiffness led to an increase of the membrane reservoir up to a maximum level, whereas in hMSCs, cytoskeleton-membrane interaction is weak and the major regulation mechanism of reservoir size appears to be membrane rigidity which, in turn, is controlled by cholesterol content. The percentage of the beads undergoing fluctuating motion on the cell surface after cholesterol depletion and cytoskeleton reorganization was significantly higher than that observed in control experiments for both types of cells (see Table 1).

DMSO is another strong reagent that can alter the cell mechanics by affecting the arrangement of the actin cytoskeleton, the interfacial energy between the membrane and cytoskeleton, and the stiffness of the lipid bilayer. Indeed, cell treatment with 2% DMSO dramatically increased the membrane tether length. Apparently, the effect of DMSO was very similar to the cumulative action of cytochalasin D and MβCD combined to increase the membrane reservoir size (Fig. 6). Most likely, DMSO influences both the membrane properties and actin cytoskeleton, causing an increase in the tether length. Interestingly, membrane tether behavior (tether length distribution, average plateau force) was very similar after cell treatment with either DMSO or a cytochalasin D/MβCD cocktail. One may suggest that hMSCs and fibroblasts have a similar maximum available membrane reservoir, but they use

different mechanisms to control the reservoir size, which include the membrane-cytoskeleton interaction and the membrane rigidity. This idea is further discussed in the following section.

DISCUSSION

Plasma membrane plays an important role throughout the whole life cycle of mammalian cells. It participates in the most critical cell functions including adhesion, motility, endocytosis and exocytosis, signaling, and metabolite traffic. An important parameter maintained by multifactor membrane homeostasis is the membrane tension. It is known to be involved in regulation of many cellular processes and should be maintained at a constant level in the range 0.001–0.1 mN/m for different cell types during various chemical and mechanical perturbations experienced by the cell (12). For example, significant variations in the cell morphology or osmolarity do not usually cause considerable changes in the membrane tension (22). However, biological membranes stretch elastically only by 2%–4% before they rupture (43). Cells must have some protective mechanisms to avoid sudden changes in tension up to lytic values of 1–10 mN/m. The ability of cells to resist fast changes in the membrane tension may be explained by a small bilayer reservoir that can buffer minor increases in the membrane tension. More dramatic and slower changes in the cell environment are further accommodated by other tension-sensitive surface area regulation mechanisms (12).

The nature of such a reservoir remains unclear, however. The anatomical basis for this reservoir may be various undulations of the membrane that flatten when tension increases. The reservoir may be represented by filopodia in migrating neuronal growth cones and fibroblasts, surface folds in macrophages, water channel-laden vesicles in rat kidney cells, and open cannicular system channels in platelets. Membrane invaginations such as coated pits and caveolae are good candidates to represent the membrane reservoir in cells with ''smooth'' surface-like fibroblasts (44). These structures are involved in many cell functions commonly associated with and controlled by the membrane reservoir (45). Membrane proteins are very likely to play a role in reservoir regulation. Physical coupling between integral membrane protein and biological membranes may induce local changes in bilayer curvature that give rise to bending moments and deformations of the membrane (46).

Although previous studies proved the existence of a membrane reservoir, few attempts have been made to characterize it quantitatively (21). Tether extraction with LOT is an excellent approach to measure the membrane reservoir size and to study quantitatively and selectively the regulatory mechanisms in different cell types. Direct evidence for existence of such a reservoir is provided by a plateau in the force-length profiles of tether extraction from live cells. Tethers are hollow thin membrane cylinders extending from the plasma membrane. In our experiments, the tether radius estimated from bright-field images was $\sim$0.2 μm, consistent with observations for other studies (23). To extract these membrane tethers we used 0.5 μm diameter latex beads. Each bead coated with antibodies against integrins typically binds several integrin molecules on the cell surface. The advantage of using small beads is to minimize cell activation associated with integrin cross-linking and binding to the bead surface. Besides, small bead size also minimizes mechanical perturbation from the initial membrane-cytoskeleton separation at the site of bead attachment to the membrane. Indeed, pulling a tether 10 μm long and 0.2 μm thick requires $\sim$6 μm^2 of membrane area. A comparable or even a larger area would be occupied by a 2 μm bead attached to the membrane. Choosing a small probe should prevent potential bead-size induced artifacts. Note that larger optical forces may be applied by LOT to bigger particles (47), but 10 pN exerted on a 0.5 μm bead was enough to form membrane tethers. Unfortunately, significant force fluctuations during tether extraction did not allow us to detect statistically significant differences between low (2–3 pN) plateau forces in cells treated with various chemicals. Stiffer optical traps should be used to study the effect of different drugs on tether force.

Based on evidence of unique biomechanical characteristics of hMSCs, we explored the membrane reservoir properties of these cells by the LOT technique. Because these cells are known to differentiate in many types of connective tissues, we used fibroblasts to compare differences in the membrane dynamics of undifferentiated and fully specialized cells. Our findings indicate considerable differences in the membrane reservoir in two types of cells. First, the membrane reservoir size appears to be more than three times larger in hMSCs than in fibroblasts. It should be noted, however, that hMSCs cultured onto 2D substrate are physically bigger than fibroblasts. If the membrane reservoir is continuously distributed on the cell surface (21), difference in the cell size may at least partially account for differences in the membrane reservoir size. More dramatic changes in the hMSC morphology during subculturing on 2D substrate may require a larger membrane buffering reservoir capacity. This can also contribute to a bigger reservoir size in stem cells. Second, differences in the membrane reservoir size in hMSCs and fibroblasts may be attributed to differential regulation of mechanisms used by these cells to maintain the reservoir. These mechanisms include cortical cytoskeleton tension, membrane-cytoskeleton association, and plasma membrane rigidity. To explore the first two possibilities, we disrupted actin fibers using cytochalasin D. The reservoir size change in response to cytochalain D treatment was strongly dependent on cell type. In agreement with other studies (48) the tether length increased substantially in fibroblasts, showing the important role of cytoskeleton in maintaining the membrane reservoir. As was reported by other authors, there is a strong association between the plasma membrane and cytoskeleton in fibroblasts (17). This interaction is mostly mediated by multiple attachments of

intracellular structural proteins to the bilayer surface rather than the few strong contacts between the membrane and cytoskeleton. This is consistent with the idea that the organization of actin cytoskeleton in fibroblasts as an extensive thin meshwork provides multiple binding sites for the lipid bilayer. The sum of many weak interactions forms a strong membrane-cytoskeleton linkage. On the other hand, hMSCs have a quite different actin cytoskeleton organization than fibroblasts, such as thick actin stress fibers and rigid stress fibers connected to the plasma membrane at a few discreet sites (e.g., focal adhesions). The overall strength of this coupling is less than that found in fibroblasts. In hMSCs the tether length almost did not change after decreasing cytoskeleton structural integrity. This suggests a much weaker membrane-cytoskeleton interaction and consequently a lesser regulatory role of cytoskeleton for the plasma membrane in hMSCs.

The effective membrane tension γ that includes the in-plane tension of bilayer and interfacial energy of membrane-cytoskeleton adhesion may be estimated from the force applied to the tether F and its radius R (23):

$$\gamma = \frac{F}{4\pi R}.$$

The tether radius was roughly assessed from bright-field images, and the effective membrane tension value was ~1.5 μN/m. This value is comparable to the resting tension in growth cones of chick neurons (3 μN/m) (23) but lower than the tension in normal molluscan neurons (40 μN/m) (22). However, from this formula alone one cannot estimate directly the contributions of the in-plane tension and membrane-cytoskeleton interaction.

The second prospective mechanism to control the apparent membrane reservoir size is the stiffness of plasma membrane itself. Cholesterol plays an important role in determining this membrane rigidity. It has been shown repeatedly that cholesterol depletion decreases the stiffness of lipid bilayer membranes (40,41). Thus, we used a cholesterol depletion approach to study the effect of membrane rigidity on the tether length. Cholesterol depletion did increase reservoir size in both types of cells. However, based on the combined treatment with cytochalasin D and MβCD, the effects of cholesterol and cytoskeleton disruption on the tether length are additive in fibroblasts. In contrast, only the membrane stiffness but not interaction with cytoskeleton predominantly determines the tether length in hMSCs. Interestingly, the plasma membrane pits' caveolae, a possible anatomical source of the membrane reservoir, are closely linked to the cholesterol level in mammalian cells. The assembly and density of these structures are related to the membrane's cholesterol concentration (49,50). Caveolae could take part in an intricate interplay between signal transduction, membrane tension regulation, and cholesterol content balance.

Another strong chemical agent that can change the mechanical properties of cells and cell membranes is DMSO, which may affect the plasma membrane reservoir size through different mechanisms by modulating the lipid bilayer and actin network mechanics. DMSO is a strong amphiphilic solvent and would readily dissolve the lipid membrane, thus directly changing its elastic properties. DMSO can also affect the arrangement of cytoskeleton and thereby increase apparent reservoir size. In addition, DMSO might indirectly affect the membrane mechanics through an alteration in the interfacial energy between the membrane and actin cytoskeleton. The overall effect of DMSO was equivalent to the concomitant cell treatment with cytochalasin D and MβCD, which supports the notion of all three mechanisms for tether length modulation by DMSO.

Together with previous findings, we propose that the two major biophysical mechanisms involved in the membrane reservoir regulation include membrane-cytoskeleton association and membrane rigidity. This postulate is supported by the fact that cytoskeleton disruption and cholesterol depletion (either with combined cytochalasin D/MβCD or DMSO treatment) induced the similar tether length in both cell types. However, there may be other factors affecting the membrane reservoir size, membrane tension, metabolism, and functions. As shown in this study, these additional mechanisms likely depend on the cell type, specialization, and cell functions in the organism. Thus, the major role of cytoskeleton in regulation of the membrane mechanical properties of fibroblasts is not surprising considering continual mechanical stress experienced by these cells. In hMSCs, however, high sensitivity to multiple environmental biochemical cues relies on increased signaling and associated transmembrane traffic that apparently require different membrane properties than fully differentiated fibroblasts. For example, tight membrane coupling to cytoskeleton may interfere with transmembrane trafficking and decrease endocytosis rates. Stem cells therefore may rely on the membrane stiffness to regulate the membrane reservoir size and membrane tension. This unique and outstanding membrane mechanics may have great implications for stem cell differentiation pathways.

SUMMARY

The membrane mechanical properties of hMSCs were studied with the LOT technique. Much longer tethers were extracted from the hMSC plasma membrane compared to fully differentiated fibroblasts. Different membrane mechanics is attributed to differential membrane-cytoskeleton interaction in these two types of cells. Our results support the hypothesis that the membrane reservoir buffers variations in the membrane surface tension. Two major mechanisms for membrane regulation include 1), membrane stiffness, and 2), its interaction with cytoskeleton. Whereas fibroblasts use both mechanisms, hMSC membrane dynamics is virtually unaffected by actin cytoskeleton. The distinctive mechanical properties of stem cell membranes are likely due to weak interaction with cytoskeleton. The cell type-specific mechanical properties of the membrane are based apparently on

particular functions of cells terminally committed to a particular lineage. Additional studies are needed to fully elucidate the membrane dynamics during stem cell differentiation, however. Because the stem cell membrane is expected to mediate highly dynamic responses to multiple signals and environmental stimuli in morphogenesis, tissue remodeling, and commitment to specialized cell phenotypes, detailed characterization of the different mechanical features of stem cells may help to provide new effective approaches in stem cell-based tissue engineering and regenerative medicine.

REFERENCES

1. Kassem, M. 2004. Mesenchymal stem cells: biological characteristics and potential clinical applications. *Cloning Stem Cells.* 6:369–374.

2. Barry, F. P., and J. M. Murphy. 2004. Mesenchymal stem cells: clinical applications and biological characterization. *Int. J. Biochem. Cell Biol.* 36:568–584.

3. Minguell, J. J., A. Erices, and P. Conget. 2001. Mesenchymal stem cells. *Exp. Biol. Med. (Maywood).* 226:507–520.

4. Le Blanc, K. 2003. Immunomodulatory effects of fetal and adult mesenchymal stem cells. *Cytotherapy.* 5:485–489.

5. Settleman, J. 2004. Tension precedes commitment—even for a stem cell. *Mol. Cell.* 14:148–150.

6. Thomas, C. H., J. H. Collier, C. S. Sfeir, and K. E. Healy. 2002. Engineering gene expression and protein synthesis by modulation of nuclear shape. *Proc. Natl. Acad. Sci. USA.* 99:1972–1977.

7. Rodriguez, J. P., M. Gonzalez, S. Rios, and V. Cambiazo. 2004. Cytoskeletal organization of human mesenchymal stem cells (MSC) changes during their osteogenic differentiation. *J. Cell. Biochem.* 93: 721–731.

8. McBeath, R., D. M. Pirone, C. M. Nelson, K. Bhadriraju, and C. S. Chen. 2004. Cell shape, cytoskeletal tension, and RhoA regulate stem cell lineage commitment. *Dev. Cell.* 6:483–495.

9. Emoto, K., and M. Umeda. 2001. Membrane lipid control of cytokinesis. *Cell Struct. Funct.* 26:659–665.

10. Lundbaek, J. A., P. Birn, A. J. Hansen, R. Sogaard, C. Nielsen, J. Girshman, M. J. Bruno, S. E. Tape, J. Egebjerg, D. V. Greathouse, G. L. Mattice, R. E. Koeppe 2nd, and O. S. Andersen. 2004. Regulation of sodium channel function by bilayer elasticity: the importance of hydrophobic coupling. Effects of micelle-forming amphiphiles and cholesterol. *J. Gen. Physiol.* 123:599–621.

11. Hamill, O. P., and B. Martinac. 2001. Molecular basis of mechanotransduction in living cells. *Physiol. Rev.* 81:685–740.

12. Morris, C. E., and U. Homann. 2001. Cell surface area regulation and membrane tension. *J. Membr. Biol.* 179:79–102.

13. Raucher, D., and M. P. Sheetz. 2000. Cell spreading and lamellipodial extension rate is regulated by membrane tension. *J. Cell Biol.* 148: 127–136.

14. Raucher, D., and M. P. Sheetz. 1999. Membrane expansion increases endocytosis rate during mitosis. *J. Cell Biol.* 144:497–506.

15. Togo, T., T. B. Krasieva, and R. A. Steinhardt. 2000. A decrease in membrane tension precedes successful cell-membrane repair. *Mol. Biol. Cell.* 11:4339–4346.

16. Sheetz, M. P. 2001. Cell control by membrane-cytoskeleton adhesion. *Nat. Rev. Mol. Cell Biol.* 2:392–396.

17. Raucher, D., T. Stauffer, W. Chen, K. Shen, S. Guo, J. D. York, M. P. Sheetz, and T. Meyer. 2000. Phosphatidylinositol 4,5-bisphosphate functions as a second messenger that regulates cytoskeleton-plasma membrane adhesion. *Cell.* 100:221–228.

18. Svetina, S., B. Bozic, J. Derganc, and B. Zeks. 2001. Mechanical and functional aspects of membrane skeletons. *Cell. Mol. Biol. Lett.* 6:677–690.

19. Merkel, R., R. Simson, D. A. Simson, M. Hohenadl, A. Boulbitch, E. Wallraff, and E. Sackmann. 2000. A micromechanic study of cell polarity and plasma membrane cell body coupling in Dictyostelium. *Biophys. J.* 79:707–719.

20. Dai, J., M. P. Sheetz, X. Wan, and C. E. Morris. 1998. Membrane tension in swelling and shrinking molluscan neurons. *J. Neurosci.* 18: 6681–6692.

21. Evans, E., V. Heinrich, F. Ludwig, and W. Rawicz. 2003. Dynamic tension spectroscopy and strength of biomembranes. *Biophys. J.* 85: 2342–2350.

22. Raucher, D., and M. P. Sheetz. 1999. Characteristics of a membrane reservoir buffering membrane tension. *Biophys. J.* 77:1992–2002.

23. Hochmuth, F. M., J. Y. Shao, J. Dai, and M. P. Sheetz. 1996. Deformation and flow of membrane into tethers extracted from neuronal growth cones. *Biophys. J.* 70:358–369.

24. Sheetz, M. P., editor. 1998. Laser Tweezers in Cell Biology. Academic Press, San Diego, CA.

25. Fallman, E., S. Schedin, J. Jass, M. Andersson, B. E. Uhlin, and O. Axner. 2004. Optical tweezers based force measurement system for quantitating binding interactions: system design and application for the study of bacterial adhesion. *Biosens. Bioelectron.* 19:1429–1437.

26. Li, Z., B. Anvari, M. Takashima, P. Brecht, J. H. Torres, and W. E. Brownell. 2002. Membrane tether formation from outer hair cells with optical tweezers. *Biophys. J.* 82:1386–1395.

27. Neuman, K. C., and S. M. Block. 2004. Optical trapping. *Rev. Sci. Instrum.* 75:2787–2809.

28. Kucik, D. F., T. E. O'Toole, A. Zheleznyak, D. K. Busettini, and E. J. Brown. 2001. Activation-enhanced $\alpha_{IIb}\beta_3$-integrin-cytoskeleton interactions outside of focal contacts require the α-subunit. *Mol. Biol. Cell.* 12:1509–1518.

29. Jin, T., and J. Li. 2002. Dynamitin controls Beta 2 integrin avidity by modulating cytoskeletal constraint on integrin molecules. *J. Biol. Chem.* 277:32963–32969.

30. Ermilov, S. A., D. R. Murdock, D. El-Daye, W. E. Brownell, and B. Anvari. 2005. Effects of salicylate on plasma membrane mechanics. *J. Neurophysiol.* 94:2105–2110.

31. Peterman, E. J., F. Gittes, and C. F. Schmidt. 2003. Laser-induced heating in optical traps. *Biophys. J.* 84:1308–1316.

32. Tsukita, S., and S. Yonemura. 1999. Cortical actin organization: lessons from ERM (ezrin/radixin/moesin) proteins. *J. Biol. Chem.* 274:34507–34510.

33. Feneberg, W., M. Aepfelbacher, and E. Sackmann. 2004. Microviscoelasticity of the apical cell surface of human umbilical vein endothelial cells (HUVEC) within confluent monolayers. *Biophys. J.* 87:1338–1350.

34. Ingber, D. E. 2003. Tensegrity I. Cell structure and hierarchical systems biology. *J. Cell Sci.* 116:1157–1173.

35. Sultan, C., D. Stamenovic, and D. E. Ingber. 2004. A computational tensegrity model predicts dynamic rheological behaviors in living cells. *Ann. Biomed. Eng.* 32:520–530.

36. Barenholz, Y. 2004. Sphingomyelin and cholesterol: from membrane biophysics and rafts to potential medical applications. *Subcell. Biochem.* 37:167–215.

37. Silvius, J. R. 2003. Role of cholesterol in lipid raft formation: lessons from lipid model systems. *Biochim. Biophys. Acta.* 1610: 174–183.

38. Kwik, J., S. Boyle, D. Fooksman, L. Margolis, M. P. Sheetz, and M. Edidin. 2003. Membrane cholesterol, lateral mobility, and the phosphatidylinositol 4,5-bisphosphate-dependent organization of cell actin. *Proc. Natl. Acad. Sci. USA.* 100:13964–13969.

39. Christian, A. E., M. P. Haynes, M. C. Phillips, and G. H. Rothblat. 1997. Use of cyclodextrins for manipulating cellular cholesterol content. *J. Lipid Res.* 38:2264–2272.

40. Needham, D., and R. S. Nunn. 1990. Elastic deformation and failure of lipid bilayer membranes containing cholesterol. *Biophys. J.* 58:997–1009.

41. Subczynski, W. K., and A. Wisniewska. 2000. Physical properties of lipid bilayer membranes: relevance to membrane biological functions. *Acta Biochim. Pol.* 47:613–625.

42. Hao, M., S. Mukherjee, and F. R. Maxfield. 2001. Cholesterol depletion induces large scale domain segregation in living cell membranes. *Proc. Natl. Acad. Sci. USA.* 98:13072–13077.

43. Waugh, R. E. 1983. Effects of abnormal cytoskeletal structure on erythrocyte membrane mechanical properties. *Cell Motil.* 3:609–622.

44. Anderson, R. G. 1998. The caveolae membrane system. *Annu. Rev. Biochem.* 67:199–225.

45. Cohen, A. W., R. Hnasko, W. Schubert, and M. P. Lisanti. 2004. Role of caveolae and caveolins in health and disease. *Physiol. Rev.* 84:1341–1379.

46. Sens, P., and M. S. Turner. 2004. Theoretical model for the formation of caveolae and similar membrane invaginations. *Biophys. J.* 86:2049–2057.

47. Wright, W. H., G. J. Sonek, and M. W. Berns. 1994. Parametric study of the forces on microspheres held by optical tweezers. *Appl. Opt.* 33:1735–1748.

48. Dai, J., and M. P. Sheetz. 1995. Mechanical properties of neuronal growth cone membranes studied by tether formation with laser optical tweezers. *Biophys. J.* 68:988–996.

49. Ikonen, E., and R. G. Parton. 2000. Caveolins and cellular cholesterol balance. *Traffic.* 1:212–217.

50. Kurzchalia, T. V., and R. G. Parton. 1999. Membrane microdomains and caveolae. *Curr. Opin. Cell Biol.* 11:424–431.